ORIGINAL ARTICLE

Benzene sorption complex of fully dehydrated fully Mn²⁺-exchanged zeolite Y (FAU) and its single-crystal structure

Md. Shamsuzzoha · Sung Man Seo ·
Young Hun Kim · Woo Taik Lim

Abstract The single-crystal structure of a benzene sorption complex of fully dehydrated fully Mn²⁺-exchanged zeolite Y, $|Mn_{37.5}(C_6H_6)_{24}|[Si_{117}Al_{75}O_{384}]$-FAU, has been determined by single-crystal synchrotron X-ray diffraction techniques in the cubic space group $Fd\bar{3}m$ at 100(1) K. A fully dehydrated and fully Mn²⁺-exchanged zeolite Y ($|Mn_{37.5}|[Si_{117}Al_{75}O_{384}]$-FAU, Si/Al = 1.56) was treated with zeolitically dried benzene at 297(1) K for 3 days. The structure was refined using all intensities to the final error indices (using the 544 reflections for which $F_o > 4\sigma(F_o)$) $R_1 = 0.050$ (based on F) and $wR_2 = 0.147$ (based on F^2). In this structure, Mn²⁺ ions occupy four crystallographic sites: 13.5 Mn²⁺ ions are at the centers of the double 6-rings; 4 Mn²⁺ ions are in the sodalite cavity opposite to the double 6-rings; the remaining 20 Mn²⁺ ions are found at two non-equivalent threefold axes in the sodalite cavity and supercage with occupancies of 2 and 18, respectively. The 24 benzene molecules are found at two distinct positions within the supercages. Eighteen benzene molecules are found on the threefold axes in the supercages where each interacts facially with one of site-II Mn²⁺ ions (Mn²⁺-benzene center = *ca.* 2.53 Å). The remaining six benzene molecules lie on the planes of the 12-rings where each is stabilized by multiple weak electrostatic and van der Waals interactions with framework oxygens.

Introduction

Zeolites are extremely useful for commercial application as catalysts for several important reactions including cracking, isomerization, and hydrocarbon synthesis and for specific high yield rearrangement reactions involving hydrocarbons and other organic molecules [1]. Exchangeable transition-metal ions in zeolites are generally coordinatively unsaturated, which are able to catalyze reduction, oxidation, and carbonylation reactions [2].

E. Diaz et al. [3] investigated the adsorptions of several alkanes, cyclic hydrocarbons, aromatic hydrocarbons, and chlorinated compounds on Na, Ca, Co, Mn, and Fe-exchanged zeolites A and X as adsorbents. Adsorption parameters, dispersive surface energy interaction, and specific interaction parameters were determined for each solute-adsorbent system by inverse gas chromatography (IGC). They found that adsorption properties depend on what cation was exchanged; Mn, Na–X and Co, Na–X zeolites exhibited the strongest interactions with benzene due to their higher adsorption enthalpies.

The sorption of hydrocarbons into zeolites has been studied by a variety of techniques, especially X-ray diffraction [4], neutron diffraction [5], and infrared spectroscopy [6]. These studies have provided detailed information about the sorption sites of organic molecules and inaccessibility of some molecules at specific sites in zeolite framework.

Md. Shamsuzzoha · S. M. Seo · W. T. Lim (✉)
Department of Applied Chemistry, Andong National University, Andong 760-749, Korea
e-mail: wtlim@andong.ac.kr

Y. H. Kim
Department of Environmental Engineering, Andong National University, Andong 760-749, Korea

In the recent years, the structures of organic sorption complexes of transition-metal ion-exchanged zeolites A and X have been investigated by several scientists. Many of the hydrocarbon sorption complexes, including C_2H_2, C_2H_4, C_3H_6, and C_6H_6, which were determined by single crystal X-ray diffraction techniques, have been summarized by K. Seff et al. [7]. Among of these, the aromatic hydrocarbon sorption on zeolites have drawn particular interest due to the utility of zeolites as molecular sieves and catalysts, and the foundation of several industrially important reactions such as toluene disproportionation, adsorptive separation of the xylene isomers, and benzene alkylation [8]. The catalytic and sorption properties of zeolites depend not only on the kinds of cations, their positions, and distribution in their dehydrated structures but also on the interactions between the cations and the sorbed molecules, the framework and sorbed molecules, and among the sorbed molecules themselves.

The location of benzene molecules in Na–Y has been determined by powder neutron diffraction techniques [9, 10]. The benzene molecules were localized on two distinct sites at 4 K; one was in the supercage near site II, and another was centered in the plane of the 12-ring window between adjacent supercages, but the benzene molecules were found only in the supercages at the room temperature.

The nature of the adsorption sites and mobility of benzene in Na–Y at room temperature were investigated by molecular dynamics calculations and the result showed a loading of two benzene molecules per supercage [11]. It was observed that benzene molecules were found near the 6-rings and in the 12-rings and could be migrated from one adsorption site to another.

Benzene molecules were also found at two distinct sites in the structures of Ca_{46}–X·$28C_6H_6$ [12], Cd_{46}–X·$43C_6H_6$ [13], and $Sr_{37.5}$–Y·$33C_6H_6$ [14] by single-crystal X-ray diffraction techniques. The influence of the temperature on sorption of benzene in K, Ca, and Sr-exchanged zeolites Y was investigated by high-speed X-ray powder diffraction method [15]; the influence of benzene molecules on the cation distribution rapidly increased with the cation-molecule interaction energy. The sorption behavior of benzene on dehydrated Na-Y has been studied by ^{129}Xe, ^1H, and ^{13}C NMR [16]; the maximum number of benzene molecules that could be occupied within a supercage of zeolite was found to lie between 4.9 and 5.2.

D. Barthomeuf et al. investigated the change of location of benzene in faujasite-type zeolite upon coadsorption of NH_3 or HCl. Their study by infrared spectroscopy showed that a coadsorbate such as NH_3 or HCl able to interact more strongly than benzene with the cations or the framework oxygen could displace benzene to the other sites [17].

M. Czjzek et al. studied the structures of Yb, Na–Y zeolites containing sorbed perdeuterated xylenes by powder neutron diffraction technique [18]. They reported that the xylene molecules were located in the supercage, the plane of the aromatic ring being perpendicular to the threefold axis with short contacts to the Na^+ cations at site II′.

Perdeuterobenzene sorption structure in zeolite H-SAPO-37 was investigated by powder neutron diffraction and ^2H NMR techniques [19]. The diffraction measurements revealed that benzene was located both above the 6-ring window and in the plane of the 12-ring window at 5 K.

The benzene sorption complex of Mn_{46}-X [20] was prepared by treating with zeolitically dried benzene for 2 days and its structure was determined by single crystal X-ray diffraction technique. In this structure, 16 Mn^{2+} ions filled site I as in dehydrated Mn_{46}–X and 30 Mn^{2+} ions at site II were split crystallographically into two positions with occupancies of 26 and 4 [21]. The benzene molecules were found at two sites within the supercages. The 26 benzene molecules lie on threefold axes in the large cavities, where they interacted facially with 26 Mn^{2+} ions; the other 14 benzene molecules were found in the planes of the 12-rings, where they were stabilized by multiple van der Waals forces and electrostatic interactions.

This work was initiated to investigate the sorption property of benzene within Mn^{2+}-exchanged zeolite Y (Si/Al = 1.56), to determine the positions of the sorbed benzene molecules, and to observe the cation shifts upon sorption and the cation-sorbate interactions by single-crystal X-ray diffraction techniques. Mn^{2+}-exchanged zeolite Y was chosen due to strong interaction with benzene molecules.

Experimental section

Crystal preparation

Large colorless single crystals of sodium zeolite Y, stoichiometry $Na_{75}Si_{117}Al_{75}O_{384}$, with diameters up to 0.32 mm were prepared in the laboratory of Nano Material Structure Research, Andong National University, Korea [22]. Crystals of hydrated $Mn_{37.5}$–Y (or Mn–Y) were prepared by static ion-exchange of Na_{75}–Y with aqueous 0.1 M $Mn(NO_3)_2·xH_2O$ (Aldrich, 99.99%). The 0.1 g of hydrated sodium zeolite Y was mixed with 10 mL of 0.1 M $Mn(NO_3)_2$ in 15-mL conical tube and then the mixture was stirred on a shaking incubator at 343 K for 24 h. The ion-exchange procedure was repeated 20 times with the fresh $Mn(NO_3)_2$ solution. The product was then washed each time with 300-mL distilled water followed by filtration and oven-dried at 323 K for 1 day. One of these, clear and brick brown color octahedron about 0.31 mm in cross section hydrated Mn^{2+}-exchanged zeolite Y crystal was

lodged in a fine Pyrex capillary. The capillary containing the crystal was attached to a vacuum system, and the crystal was cautiously dehydrated by gradually increasing its temperature (*ca.* 25 K/h) to 723 K at a constant pressure of 1×10^{-6} Torr. The system was kept at the final dehydration status for 48 h. While these conditions were maintained, the hot contiguous downstream length of the vacuum system, including two sequential U-tubes of zeolite 5A beads fully activated in situ, was cooled to an ambient temperature to prevent the movement of water molecules from more distant parts of the vacuum system to the crystals. Still under vacuum in the capillary, the crystal was then allowed to cool at room temperature; the crystal had pale brown color. To prepare the benzene sorption complex, the crystal was treated with zeolitically dried benzene for 3 days at 297(1) K, and then evacuated for 5 h at this temperature and pressure was found at 9×10^{-6} Torr. It was then sealed in its capillary by torch and removed from the vacuum line. Microscopic examination showed that the crystals had pale brown color.

Single-crystal X-ray diffraction work

X-ray diffraction data of the resulting single-crystal was collected at 100(1) K using an ADSC Quantum210 detector at Beamline 6B MXI in The Pohang Light Source. The crystal evaluation and data collection were done using 0.9000 Å wavelength of X-radiation with a detector-to-crystal distance of 6.0 cm. Preliminary cell constants and an orientation matrix were determined from 72 sets of frames collected at scan intervals of 5° with an exposure time of 10 s per frame. The basic scale file was prepared using the HKL2000 program [23]. The reflections were successfully indexed by the automated indexing routine of the DENZO program [23]. The total reflections were harvested by collecting 72 sets of frames with 5° scans with an exposure time of 10 s per frame. These highly redundant data sets were corrected for Lorentz and polarization effects, and (negligible) corrections for crystal decay were also applied. The space group $Fd \bar{3}m$ was determined by the program XPREP [24]. The summary of the experimental and crystallographic data is presented in Table 1.

Structure determination

Full-matrix least-squares refinement using SHELXL97 [25] was done on F_o^2 using all data for the crystal. Refinement was initiated with the atomic parameters of the framework atoms [(Si,Al), O(1), O(2), O(3), and O(4)] in dehydrated $|Mn_{37.5}|[Si_{117}Al_{75}O_{384}]$-FAU [26]. Anisotropic refinement converged to an unweighted R_1 index

Table 1 Summary of experimental and crystallographic data

$|Mn_{37.5}(C_6H_6)_{24}|[Si_{117}Al_{75}O_{384}]$-FAU	
Crystal cross-section (mm)	0.31
Ion exchange T (K)	343
Ion exchange for Mn^{2+} (day, mL)	20, 200
Dehydration T (K)	723
Crystal color	Pale brown
Data collection T (K)	100(1)
Space group, Z	$Fd \bar{3}m$, 1
X-ray source	PLS (6B MXI BL)
Wavelength (Å)	0.90000
Unit cell constant, a (Å)	24.5810(10)
2θ range in data collection (deg)	60.62
No. of unique reflections, m	572
No. of reflections with $F_o > 4\sigma(F_o)$	544
No. of variables, s	61
Data/parameter ratio, m/s	9.38
Weighting parameters, a/b	0.064/326.7
Final error indices	
$R_1/wR_2(F_o > 4\sigma(F_o))^a$	0.0500/0.1471
R_1/wR_2(all intensities)^b	0.0522/0.1536
Goodness-of-fit^c	1.260

^{a} $R_1 = \Sigma|F_o-|F_c||/\Sigma F_o$ and $wR_2 = [\Sigma w(F_o^2-F_c^2)^2/\Sigma w(F_o^2)^2]^{1/2}$; R_1 and wR_2 are calculated using only the 544 reflections for which $F_o > 4\sigma(F_o)$

^{b} R_1 and wR_2 are calculated using all 572 unique reflections measured

^{c} Goodness-of-fit = $(\Sigma w(F_o^2-F_c^2)^2/(m-s))^{1/2}$, where m and s are the number of unique reflections and variables, respectively

$(\Sigma|F_o-|F_c||/\Sigma F_o)$, of 0.4393 and a weighted R_2 index, $([\Sigma w(F_o^2-F_c^2)^2/\Sigma w(F_o^2)^2]^{1/2})$, of 0.8172 and are calculated using only the 544 reflections for which $F_o > 4\sigma(F_o)$.

A difference Fourier function showed the largest peak, at (0.0, 0.0, 0.0) with peak height 24.2 $e\text{Å}^{-3}$. Refinement including it as Mn^{2+} ion with fixed isotropic temperature factor at Mn(1) converged to $R_1 = 0.329$ and $wR_2 = 0.762$. The progress of structure determination as subsequent peaks at (0.0649, 0.0649, 0.0649), (0.2085, 0.2085, 0.2085), and (0.2314, 0.2314, 0.2314) were found on difference Fourier functions with peak height of 3.2, 1.9, and 15.9, $e\text{Å}^{-3}$, respectively, and identified as non-framework atoms is given in Table 3. The refinement with three additional peaks from Fourier difference functions at Mn(1′), Mn(2′), and Mn(2) and anisotropic thermal parameters to refine the framework atoms led to convergence with $R_1 = 0.098$ and $wR_2 = 0.297$.

A subsequent deference Fourier synthesis revealed a peak of height, 1.59 $e\text{Å}^{-3}$, at the general position (0.2500, 0.2904, 0.3316). Least-squares refinement including this peak as C(1) with an isotropic temperature factor converged to $R_1 = 0.075$ and $wR_2 = 0.208$. A later difference

Fourier synthesis indicated with a peak of height, 1.58 eÅ^{-3}, that the remaining carbon atoms of these benzene molecules were at (0.2283, 0.2283, 0.4549). Least squares refinement including this peak as C(2) with isotropic thermal parameter converged to $R_1 = 0.059$ and $wR_2 = 0.169$.

The occupancies at Mn(1), Mn(1′), Mn(2′), Mn(2), and C(1) were fixed as shown in Table 3 by the assumption stoichiometry, the requirement of neutrality, and the observation that the occupancies at Mn(2) and C(1) were refined with the ratio of 1:6. It is assumed that one benzene molecule(C_6H_6) is associated with each Mn(2), the reason of such coordination is that each Mn(2) ion has moved 0.44 Å more into the supercage as compared to its position in the dehydrated $Mn_{37.5}$–Y structure [26]. The anisotropic refinement of the C atoms at C(1) and C(2) converged to $R_1 = 0.051$ and $wR_2 = 0.151$. The hydrogen atoms were simulated and then refined.

The final cycles of refinement were done with anisotropic temperature factors for framework atoms, all Mn^{2+} ions, and C atoms with the final weighting-scheme parameters, converged to $R_1 = 0.050$ and $wR_2 = 0.147$. Table 2 is presented for the steps of structure determination and

refinements as new atomic positions were found on successive difference-Fourier electron-density functions. All shifts in the final cycles of refinement were less than 0.1% of their corresponding estimated standard deviations. Atomic scattering factors for Mn^{2+}, O^-, C, and (Si,Al) were used [27, 28]. All scattering factors were modified to account for anomalous dispersion [29, 30]. The final structural parameters, selected interatomic distances, and angles are presented in Tables 3, 4, and 5, respectively.

Results

The framework structure of faujasite consists of the double 6-ring (D6R, hexagonal prism), the sodalite cavity (a cubooctahedron) connected in such a way that they create an open three dimensional pore system with large supercages capable of hosting hydrocarbons, accessible via 12-membered ring windows [31] (Fig. 1). Each unit cell has 8 supercages, 8 sodalite cavities, 16 double 6-rings (D6Rs), 16 12-rings, and 32 single 6-rings (S6Rs).

Table 2 Steps of structure determination as atom positions are found

Step	Occupancy[a]						R_1	wR_2
	Mn(1)	Mn(1′)	Mn(2′)	Mn(2)	C(1)	C(2)		
1[b]							0.4393	0.8172
2[c]	8.8(8)						0.3136	0.7597
3[c,d]	12.9(8)						0.3289	0.7620
4[c]	13.9(4)			14.0(5)			0.1233	0.4878
5[c]	13.2(4)	12.9(13)		17.6(5)			0.1001	0.2883
6[c,e]	13.2(4)	12.7(13)	1.2(4)	17.2(5)			0.0981	0.2967
7[c]	14.3(3)	3.8(5)	1.8(4)	16.8(4)	105(5)		0.0747	0.2083
8[c]	13.4(2)	3.8(4)	2.5(3)	17.5(3)	132(6)	42(3)	0.0591	0.1694
9[f,c]	13.4(2)	3.7(4)	2.3(3)	17.9(3)	108(2)	36(3)	0.0597	0.1702
10[g]	13.4(2)	3.7(4)	2.1(3)	18.1(3)	109(2)	36(3)	0.0567	0.1625
11[h,g]	13.5	4	2	18	108	36	0.0566	0.1622
12[i,g]	13.5	4	2	18	108	36	0.0512	0.1512
13[j,g]	13.5	4	2	18	108	36	0.0500	0.1471

[a] The Occupancy is given as the number of Mn^{2+} ions per unit cell

[b] Only the atoms of zeolite framework were included in the initial structure model. Framework atoms were allowed to refine anisotropically

[c] Isotropic temperature factors were used for all Mn^{2+} positions

[d] Fixed isotropic thermal parameter for Mn(1) at 0.05

[e] Fixed isotropic thermal parameter for Mn(2′) at 0.05

[f] Constraint work was done between Mn(2) and C(1)

[g] All Mn^{2+} ions were refined anisotropically

[h] All atoms were fixed

[i] Carbon atoms were refined anisotropically

[j] Hydrogen atom of Benzene were simulated

Table 3 Positional, thermal, and occupancy parameters[a]

Atom	Wyckoff position	Cation site	x	y	z	U_{11} [b]	U_{22}	U_{33}	U_{23}	U_{13}	U_{12}	Occupancy[c]		
												Initial	Varied	Fixed
Si,Al	192(i)		−532(1)	1226(1)	358(1)	150(8)	108(8)	124(8)	−17(5)	1(5)	4(5)	192		
O(1)	96(h)		−1076(1)	0	1076(1)	235(17)	199(26)	235(17)	−52(14)	14(21)	52(14)	96		
O(2)	96(g)		−23(1)	−23(1)	1469(2)	200(16)	200(16)	225(27)	38(15)	38(15)	42(21)	96		
O(3)	96(g)		−310(2)	626(1)	626(1)	193(27)	235(18)	235(18)	42(21)	51(15)	51(15)	96		
O(4)	96(g)		820(1)	820(1)	3166(2)	169(17)	169(17)	293(29)	−16(14)	−16(14)	56(20)	96		
Mn(1)	16(c)	I	0	0	0	132(8)	132(8)	132(8)	28(7)	28(7)	28(7)		13.4(2)	13.5
Mn(1')	32(e)	I'	648(6)	648(6)	648(6)	518(58)	518(58)	518(58)	171(71)	171(71)	171(71)		3.7(4)	4
Mn(2')	32(e)	II'	2046(6)	2046(6)	2046(6)	131(55)	131(55)	131(55)	−58(67)	−58(67)	−58(67)		2.1(4)	2
Mn(2)	32(e)	II	2319(1)	2319(1)	2319(1)	203(9)	203(9)	203(9)	42(9)	42(9)	42(9)		18.1(3)	18
C(1)	96(g)		2514(7)	2926(7)	3313(7)	1017(130)	1480(188)	1148(143)	−380(121)	−247(101)	−717(126)		109(2)	108
C(2)	96(g)		2286(8)	2286(8)	4535(10)	589(100)	589(100)	361(139)	−151(89)	−151(89)	92(122)		36(3)	36
H(1)[d]	96(g)		2246	2926	3580	1458							108	108
H(2)[e]	96(g)		2167	2167	4196	616							36	36
													$\Sigma Mn^{2+} = 37.3(4)$	37.5

[a] Positional parameters $\times 10^4$ and thermal parameters $\times 10^4$ are given. Numbers in parentheses are the estimated standard deviations in the units of the least significant figure given for the corresponding parameter

[b] The anisotropic temperature factor is $\exp[-2\pi^2 a^{-2}(U_{11}h^2 + U_{22}k^2 + U_{33}l^2 + 2U_{23}kl + 2U_{13}hl + 2U_{12}hk)]$

[c] Occupancy factors are given as the number of atoms or ions per unit cell

[d] These hydrogen coordinates were calculated for Benzene(1)

[e] Calculated hydrogen coordinates for benzene(2)

Table 4 Selected interatomic distances (Å) and angles (deg)[a]

(Si,Al)–O(1)	1.6422(23)
(Si,Al)–O(2)	1.6728(21)
(Si,Al)–O(3)	1.7040(24)
(Si,Al)–O(4)	1.6268(15)
Mean (Si,Al)–O	1.6615(24)
Mn(1)–O(3)	2.306(5)
Mn(1′)–O(3)	2.357(17)
Mn(2′)–O(2)	2.182(8)
Mn(2)–O(2)	2.205(5)
O(1)–(Si,Al)–O(2)	112.90(18)
O(1)–(Si,Al)–O(3)	105.88(21)
O(1)–(Si,Al)–O(4)	111.31(22)
O(2)–(Si,Al)–O(3)	106.69(21)
O(2)–(Si,Al)–O(4)	107.19(23)
O(3)–(Si,Al)–O(4)	112.87(24)
(Si,Al)–O(1)–(Si,Al)	130.7(3)
(Si,Al)–O(2)–(Si,Al)	135.1(3)
(Si,Al)–O(3)–(Si,Al)	124.6(3)
(Si,Al)–O(4)–(Si,Al)	156.7(4)
O(3)–Mn(1)–O(3)	89.75(17), 90.25(17)
O(3)–Mn(1′)–O(3)	87.3(8)
O(2)–Mn(2′)–O(2)	114.2(5)
O(2)–Mn(2)–O(2)	112.31(13)

[a] The numbers in parentheses are the estimated standard deviations in the units of the least significant digit given for the corresponding parameter

Table 5 Selected interatomic distances (Å) and angles (deg) involving sorbed benzene molecules[a]

Benzene(1)	
C(1)-C(1)	1.43(4)
C(1)–H(1)	0.930
C(1)–C(1)–C(1)	120.00(1)
Benzene(2)	
C(2)–C(2)	1.366(24)
C(2)–H(2)	0.930
C(2)–C(2)–C(2)	119.4(7)
Benzene(1)–Mn(2)	
Mn(2)–C(1)	2.904(15)
Mn(2)–center[b]	2.53
Benzene(1)–Framework	
C(1)–O(1)	3.740(18)
C(1)–O(2)	3.371(15)
C(1)–O(4)	3.700(16)
H(1)–O(1)	3.060
H(1)–O(2)	3.378
H(1)–O(4)	3.513
Benzene(2)-Framework	
C(2)–O(1)	3.831(19)
C(2)–O(4)	3.97(3)
H(2)–O(1)	3.183
H(2)–O(4)	3.042
Benzene(1)–benzene(2)	
C(1)–C(2)	3.82(3)/3.45(3)
H(1)–H(2)	2.934/2.474

[a] The numbers in parentheses are the estimated standard deviations in the units of the least significant digit given for the corresponding parameter

[b] Center of C_6H_6

The exchangeable cations that balance the negative charge of the faujasite framework are found within the zeolite's windows and cavities. They are usually found at the following sites shown in Fig. 1: Site I at the center of a D6R, site I′ in the sodalite cavity on the opposite side of either of the D6R's 6-rings from site I, site II′ inside the sodalite cavity near a single 6-ring (S6R) entrance to the supercage, site II in the supercage adjacent to a S6R, site III in the supercage opposite a sodalite four-ring, and site III′ somewhat or substantially off site III (off the twofold axis) but still on the inner surface of the supercage. The maximum occupancies at the cation sites I, I′, II, II′, and III in faujasite are 16, 32, 32, 32, and 48, respectively. Site III′ in faujasite studied using space group $Fd\bar{3}m$ has a maximum occupancy of 96 at Wyckoff positions 96(g) and 96(h) and 192 at the general Wyckoff position 192(i). Further description is available [22].

In the structure of $|Mn_{37.5}(C_6H_6)_{24}|[Si_{117}Al_{75}O_{384}]$-FAU, 37.5 Mn^{2+} ions are found at four different crystallographic sites. In comparison with fully dehydrated Mn_{46}–X [21], Mn^{2+} ions are found at only two sites I and II. In its benzene sorption, the occupancies of Mn^{2+} ions

are same, but to a lesser degree another site II was occupied (4 Mn^{2+} ions) [20]. The 13.5 Mn^{2+} ions at Mn(1) occupy site I at the center of the D6R's (Fig. 2a). The octahedral Mn(1)–O(3) bond distance, 2.306(5) Å, is just a little longer than the sum of the corresponding ionic radii, 0.80 + 1.32 = 2.12 Å [33], indicating a reasonably good fit. The 4 and 2 Mn^{2+} ions per unit cell at Mn(1′) and Mn(2′) are found in the sodalite cavity at site I′ and site II′, respectively (Figs. 2b and 3). Each Mn(1′) and Mn(2′) ion coordinates to three O(3) and O(2) framework oxygens at 2.357(17) and 2.182(8) Å, respectively. The remaining 18 Mn^{2+} ions at Mn(2) are at site II in the supercage (Fig. 4); these Mn^{2+} ions are 2.205(5) Å from their nearest three O(2) framework oxygens. The distances between Mn^{2+} ions and framework oxygens in Mn_{46}–X·$30C_2H_2$ [34], Mn_{46}–X·$30C_2H_4$ [21], Mn_{46}–X·$30C_3H_6$ [35], Mn_{46}–X·$16NO$ [36], Mn_{46}–X·$28NO_2$ [36], Mn_{46}–X·$89H_2S$ [37],
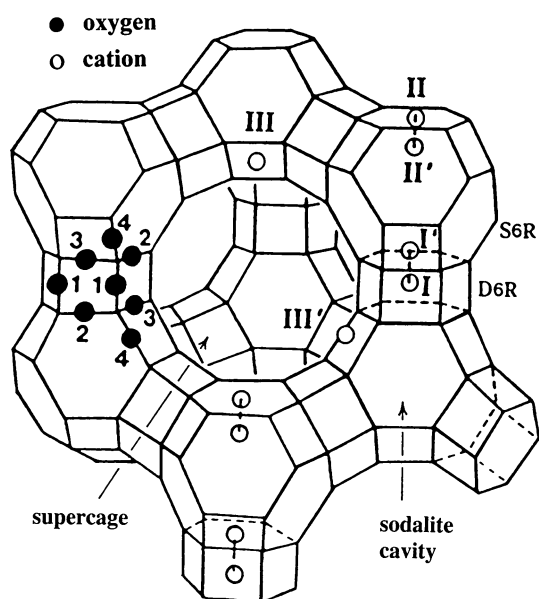
Fig. 1 Stylized drawing of the framework structure of zeolite Y. Near the center of the each line segment is an oxygen atom. The nonequivalent oxygen atoms are indicated by the numbers 1–4. There is no evidence in this work of any ordering of the silicon and aluminum atoms among the tetrahedral positions, although it is expected that Loewenstein's rule [32] would be obeyed. Extra framework cation positions are labeled with Roman numerals

and $Mn_{37.5}$–Y [26] are presented in the Table 6 to compare the distances between them in the structure of $|Mn_{37.5}(C_6H_6)_{24}|[Si_{117}Al_{75}O_{384}]$-FAU. The O(2)–Mn(2)–O(2) and O(2)–Mn(2′)–O(2) angles are $112.31(13)°$ and $114.2(5)°$, respectively (Table 4).

Crystallographically there are two kinds of benzene molecules, which are distributed at two sorption sites: (i) on a threefold axis deep inside the supercage with 108 carbon atoms (18 molecules of C_6H_6, benzene 1) per unit cell and (ii) on the 12-ring window between the supercages with 36 carbon atoms (6 molecules of C_6H_6, benzene 2) per unit cell. The 18 benzene molecules (benzene 1) at site II are bound facially to 18 Mn^{2+} ions with its aromatic ring plane nearly parallel to the 6-membered ring (Mn(2)–benzene center = 2.53 Å) (Table 5 and Figs. 3 and 4). The sorption of benzene(1) is similar argument to those observed in Na–Y [9] at a loading level of 2.6 molecules per supercage. The 6 benzene molecules per unit cell (benzene 2) are at the center of the best plane of 12-ring. These molecules are essentially bound to the framework by van der Waals forces. Benzene(2) has symmetry $\bar{3}$, so it can be generated crystallographically from a single carbon position (C(2)–C(2) = 1.366(24) Å and C(2)–C(2)–C(2) = 119.8(4)°).

Discussion

For the coordination of benzene molecules, the Mn^{2+} ions at site II have moved *ca.* 0.44 Å more into the supercage, further from their triads of three O(2) oxygens as compared with dehydrated $Mn_{37.5}$–Y [26] (Tables 7 and 8 and Figs. 3 and 4). For this movement of the Mn^{2+} ions into the supercage upon sorption, the Mn(2)–O(2) bonds have increased from 2.132(3) Å in dehydrated $Mn_{37.5}$–Y [26] to 2.205(5) Å (Table 6). The O(2)–Mn(2)–O(2) angle has corresponding decrease from near trigonal planar $(119.31(6)°)$ in dehydrated $Mn_{37.5}$–Y [26] to $112.31(13)°$ in the benzene sorption complex. These Mn^{2+} ions can coordinate more octahedrally to benzene(1) (considering benzene as tridentate). The deviation of these Mn^{2+} ions from the 6-ring plane at O(2) into the supercage is larger than those in $Mn_{37.5}$–Y [26] (Table 8).

Benzene(1) has relatively high thermal motion, but its geometry is close to ideal (C(1)–C(1) = 1.43(4) Å; C(1)–C(1)–C(1) = 120.00(1)°) (Table 5). The Carbon–Carbon distance in $C_6H_6(g)$ is 1.397(1) Å [38]. The bonding in the benzene sorption complex appears due to electrostatic interaction between the Mn^{2+} ions and the permanent electrical quadrupole moment and π electron density of the benzene molecules. The distance between benzene(1) and the framework involving the H(1)–O(1) = 3.06 Å, indicates a very weak electrostatic interaction.

The benzene(2) molecules lie on the 12-rings windows that are joint together neighboring supercages, which is formed from six O(1) atoms and six O(4) atoms linked together by Si/Al. The 12 oxygen atoms assign a close-fitting environment for the benzene molecule in the window, where its position is probably stabilized by van der Waals forces. The hydrogen atoms are directed towards the O(4) atoms and lie between the O(1) atoms, which are coplanar with the ideal benzene(2) position (Fig. 4). They have strong interactions between the hydrogens of benzene(2) and the oxygens of the 12-ring window (H(2)–O(1) = 3.183 Å and H(2)–O(4) = 3.042 Å). The benzene(2) molecules found crystallographically are close to the geometry of benzene molecule [38] (Fig. 4); the puckering of benzene(2) molecules is not crystallographically significant.

Benzene usually occupies 12-rings only at higher benzene concentrations [9, 11]. The observation of spontaneous occupation at the supercages and the 12-ring windows is an excellent agreement with the results of neutron diffraction study at 4 K [9]. The distance between C(1) of benzene(1) and C(2) of benzene(2) is 3.45(3) Å and the corresponding hydrogen distance, H(1)–H(2), is 2.474 Å. These distances indicate that clusters of benzene molecules may have formed in the supercages.

Fig. 2 Stereo views of double 6-rings (D6Rs): (**a**) 13.5 of 16 D6Rs, Mn (1) located and (**b**) 2 of 16 D6Rs, Mn(1′) located. The zeolite Y framework is drawn with heavy bonds. The coordination of Mn^{2+} ions to oxygens of the zeolite framework is indicated by light bonds. Ellipsoids of 25% probability are shown

(a)

(b)
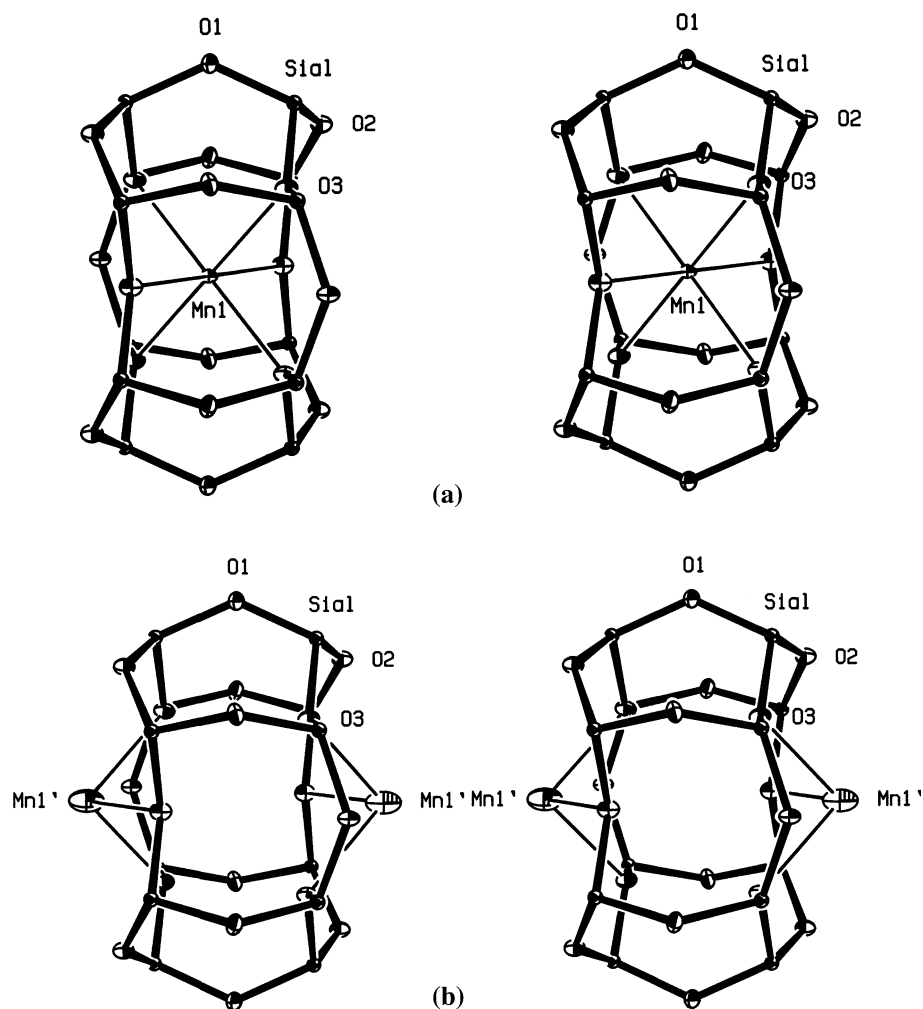
Fig. 3 A stereoview of a representative sodalite cavity. Five Mn^{2+} ions shown at Mn(1′), Mn(2′), and Mn(2). Three Mn^{2+} ions at Mn(2) coordinate to three benzene molecules. Mn(1′) and Mn(2′) do not coordinate to benzene. See the caption to Fig. 2 for other details
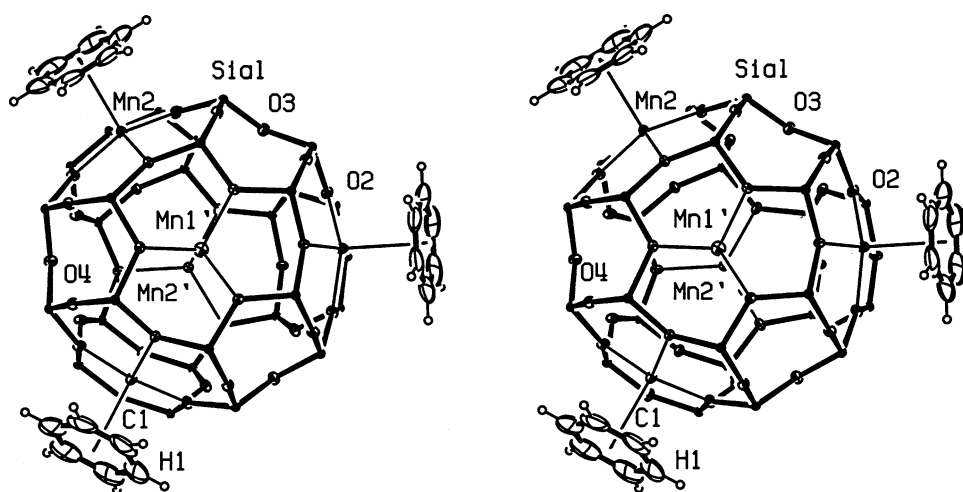
Summary

Benzene sorption complex of Fully Mn^{2+}-exchanged zeolite Y was prepared from aqueous 0.1 M $Mn(NO_3)_2 \cdot xH_2O$ solution by using static ion-exchange method at 343 K, followed by dehydration at 723 K and exposure of zeolitically dried benzene for 3 days. The structure of the benzene sorption complex of fully dehydrated and fully Mn^{2+}-

Fig. 4 Stereoview of a representative supercage. Four Mn^{2+} ions at Mn(2') and Mn(2) are shown. Each of three Mn^{2+} ions at Mn(2) coordinates to a benzene(1) molecule. The Mn^{2+} ion at Mn(2') does not coordinate to benzene. Two benzene(2) molecules are shown at 12-ring centers. See the caption to Fig. 2 for other details
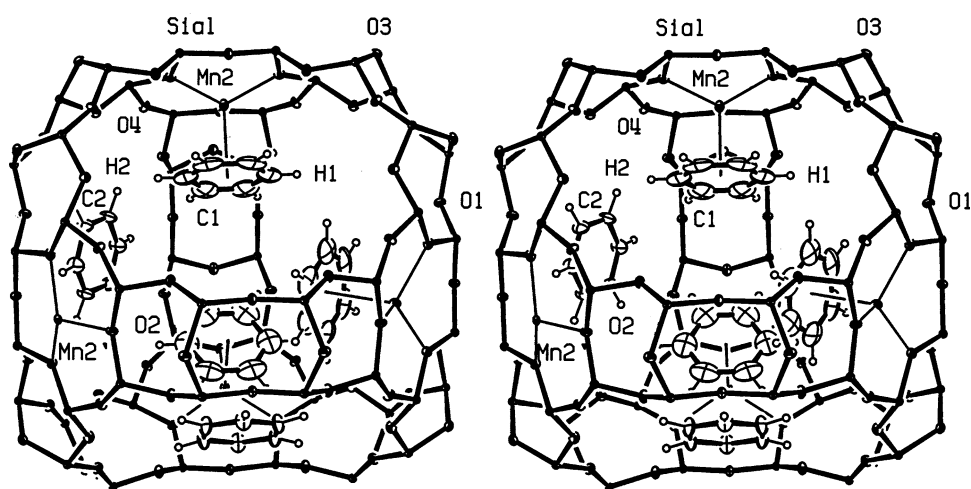
Table 6 Comparison of the distances between Mn^{2+} and its nearest framework oxygen atom

	Mn(1)–O(3)	Mn(1')–O(3)	Mn(2')–O(2)	Mn(2)–O(2)
Mn_{46}–X·$30C_2H_2$ [34]	2.290(9)	–	–	2.135(9)
Mn_{46}–X·$30C_2H_4$ [21]	2.306(13)	–	–	2.119(11)
Mn_{46}–X·$30C_3H_6$ [35]	2.290(9)	–	–	2.148(8)
Mn_{46}–X·$16NO$ [36]	2.330(16)	2.28(11)	–	2.244(15)
Mn_{46}–X·$28NO_2$ [36]	2.302(10)	2.28(4)	–	2.286(10)
Mn_{46}–X·$89H_2S$ [37]	2.285(9)	2.341(7)	2.15(2)	2.163(9)
$Mn_{37.5}$–Y [26]	2.339(3)	2.300(7)	2.219(5)	2.132(3)
$Mn_{37.5}$–Y·$24C_6H_6$ [This work]	2.306(5)	2.357(17)	2.182(8)	2.205(5)

Table 7 Displacements of atoms (Å) from 6-ring planes

	Position	Site	Displacement
At O(3)[a]	Mn(1)	I	−1.33
	Mn(1')	I'	1.42
At O(2)[b]	Mn(2')	II'	−0.53
	Mn(2)	II	0.62

[a] A positive deviation indicates that the cation lies in a sodalite cavity; a negative deviation indicates that the cation lies in a D6R (Mn(I) lies at the center of D6Rs.)

[b] A positive displacement indicates that the cation lies in a supercage; a negative deviation indicates the cation lies in a sodalite cavity

Table 8 Comparison of the deviation of site II cations and the distances of M^{2+}–C and M^{2+}–O(2) distances[a]

	M^{2+}[b]	M^{2+}–C	M^{2+}–O(2)	Ref.
Mn_{46}–X·$30C_2H_2$	0.385	2.70(5)	2.135(9)	[34]
Mn_{46}–X·$30C_2H_4$	0.38	2.76(6)	2.119(11)	[21]
Mn_{46}–X·$30C_3H_6$	0.411	2.95(9)	2.148(8)	[35]
Ca_{46}–X·$28C_6H_6$	0.55	3.14(3)	2.318(7)	[12]
Cd_{46}–X·$43C_6H_6$	0.60	3.11(5)	2.224(10)	[13]
$Mn_{37.5}$–Y[c]	0.18	–	2.132(3)	[26]
$Mn_{37.5}$–Y·$24C_6H_6$	0.62	2.908(15)	2.205(5)	This work

[a] The numbers in parentheses are the estimated standard deviations in the units of the least significant digit given for the corresponding parameter

[b] The ion or atom extends this distance into the supercage

[c] Fully dehydrated

exchanged zeolite Y was determined by single-crystal X-ray diffraction techniques. The 37.5 Mn^{2+} ions occupy at four crystallographic sites I, I', II', and II with the occupancies of 13.5, 4, 2, and 18 Mn^{2+} ions per unit cell, respectively. Two kinds of benzene molecules are found in this structure. Benzene(1) (18 molecules of benzene per unit cell) coordinates facially to 18 Mn^{2+} ions at site II in the supercage. Benzene(2) (6 molecules of benzene per unit cell) lies on the 12-ring window, where they fit well. Mn^{2+} ions at site II move more *ca.* 0.44 Å inside the supercage due to benzene sorption.

References

1. Venuto, P. B. in: Chon, H., Ihm, S.-K., Uh, Y. S., (Eds.): Structure-reactivity-selectivity relationships in reaction of organics over zeolite catalysts, Progress in Zeolite and Microporous Materials, Studies in Surface Science and Catalysis, vol. 105, p 811. Elsevier, Amsterdam (1997)

2. Cruz, W.V., Leung, P.C.W., Seff, K.: Crystal structures of nitric oxide and nitrogen dioxide sorption complexes of partially cobalt(II)-exchanged zeolite A. Inorg. Chem. **18**, 1692–1696 (1979). doi:10.1021/ic50196a059

3. Diaz, E., Ordonez, S., Vega, A., Coca, J.: Characterization of Co, Fe, and Mn-exchanged zeolites by inverse gas chromatography. J. Chromatogr. A **1049**, 161–169 (2004). doi:10.1016/j.chroma.2004.07.065

4. Amaro, A.A., Seff, K.: Crystal structure of an acetylene sorption complex of zeolite 4A. J. Phys. Chem. **77**, 906–910 (1973). doi:10.1021/j100626a010

5. Wright, P.A., Thomas, J.M., Ramdas, S., Cheetham, A.K.: Locating the sites of adsorbed species in heterogeneous catalysis: a rietveld neutron powder profile study of zenon in zeolite rho. J. Chem. Soc. Chem. Commun. **5**, 1338–1339 (1984). doi:10.1039/C39840001338

6. O'Malley, P.J.: Formation of benzene clusters in Y-type zeolites: an infrared study. Chem. Phys. Lett. **166**, 340–342 (1990). doi:10.1016/0009-2614(90)85040-J

7. Zhen, S., Seff, K.: Structures of organic sorption complexes of zeolites. Microporous Mesoporous Mater. **39**, 1–18 (2000). doi:10.1016/S1387-1811(00)00154-2

8. Song, L., Sun, Z.L., Rees, L.C.: Experimental and molecular simulation studies of adsorption and diffusion of cyclic hydrocarbons in silicalite-1. Microporous Mesoporous Mater. **55**, 31–49 (2002). doi:10.1016/S1387-1811(02)000394-3

9. Fitch, A.N., Jobic, H., Renouprez, A.: Localization of benzene in sodium-Y-zeolites by powder neutron diffraction. J. Phys. Chem. **90**, 1311–1318 (1986). doi:10.1021/j100398a021

10. Fitch, A.N., Jobic, H., Renouprez, A.: The localization of benzene in a Y-zeolite. J. Chem. Soc. Chem. Commun. 284–286 (1985). doi:10.1039/C39850000284

11. Demonis, P., Yashonath, S., Klein, M.L.: Localization and mobility of benzene in sodium-Y zeolite by molecular dynamic calculations. J. Phys. Chem. **93**, 5016–5019 (1989). doi:10.1021/j100350a003

12. Yeom, Y.H., Kim, A.N., Kim, Y., Song, S.H., Seff, K.: Crystal structure of a benzene sorption complex of dehydrated fully Ca^{2+}-exchanged zeolite X. J. Phys. Chem. **102**, 6071–6077 (1998). doi:10.1021/jp981437k

13. Kim, Y., Yeom, Y.H., Choi, E.Y., Kim, A.N., Han, Y.W.: Crystal structure of a benzene sorption complex of dehydrated fully Cd^{2+}-exchanged zeolite X. Bull. Korean Chem. Soc. **19**, 1222–1227 (1998)

14. Lee, J.M., Seo, S.M., Suh, J.M., Lim, W.T.: J. Porous Mater. (2010) (accepted)

15. Van Dun, J.J.I., Mortier, W.J., Uytterhoeven, J.B.: Influence of the temperature and the adsorption of benzene on the location of K, Ca and Sr in Y-type zeolites. Zeolites **5**, 257–260 (1985). doi:10.1016/0144-2449(85)90097-1

16. Wu, J.F., Chen, T.L., Ma, L.J., Lin, M.W., Liu, S.B.: N.m.r. investigation of benzene adsorption on a dehydrated NaY zeolite. Zeolites **12**, 86–94 (1992). doi:10.1016/0144-2449(92)90016-I

17. Mallmann, A.De, Barthomeuf, D.: Change in location of benzene in faujasite upon coadsorption of NH_3 or HCl. J. Chem. Soc. Chem. Commun, 129–130 (1989). doi:10.1039/C39890000129

18. Czjzek, M., Vogt, T., Fuess, H.: Structural evidence for pi-complexes in catalytically active Y-zeolites with o-, m-, and p-xylene. J. Phys. Chem. **95**, 5255–5261 (1991). doi:10.1021/j00166a062

19. Bull, M.L., Cheetham, A.K., Powell, B.M., Ripmeester, A.J., Ratcliffe, C.I.: The interaction of sorbates with scid sites in zeolite catalysts: A powder neutron diffraction and ^2H NMR study of benzene in H-SAPO-37. J. Am. Chem. Soc. **117**, 4328–4332 (1995). doi:10.1021/ja00120a014

20. Kim, Y., Kim, A.N., Han, Y.W., Seff, K. In: Proceedings of the 12th International Zeolites Conference, Baltimore, MD, USA, (1998)

21. Jang, S.B., Jeong, M.S., Kim, Y., Seff, K.: Crystal structures of dehydrated fully Mn^{2+}-exchanged zeolite X and of its ethylene sorption complex. J. Phys. Chem. **101**, 9041–9045 (1997). doi:10.1021/jp971671v

22. Lim, W.T., Seo, S.M., Wang, L., Lu, G.Q., Heo, N.H., Seff, K.: Single-crystal structures of highly NH_4^+-exchanged, fully deaminated, and fully Tl^+-exchanged zeolite Y (FAU, Si/Al = 1.56), all fully dehydrated. Microporous Mesoporous Mater. **129**, 11–21 (2010). doi:10.1016/j.micromeso.2009.08.028

23. Otwinowski, Z., Minor, W.: Processing of X-ray diffraction data collected in oscillation mode. Methods Enzymol. **276**, 307–326 (1997). doi:10.1016/S0076-6879(97)76066-X

24. Bruker-AXS (ver. 6.12), XPREP, Program for the automatic space group determination. Bruker AXS Inc., Madison, Wisconsin, USA (2001)

25. Sheldrick, G.M.: SHELXL97. Program for the refinement of crystal structures. University of Gottingen, Germany (1997)

26. Seo, S. M., Kim, G. H., Lim, W. T.: Investigation of distributions of Mn^{2+} ions in fully dehydrated and fully Mn^{2+}-exchanged zeolite Y, |$Mn_{37.5}$|[$Si_{117}Al_{75}O_{384}$]-FAU. Bull. Korean Chem. Soc. **31**, 2379–2382 (2010). doi:10.5012/bkcs.2010.31.8.2379

27. Doyle, P.A., Turner, P.S.: Relativistic Hartree-Fock X-ray and electron scattering factors. Acta Crystallogr. Sect. A **24**, 390–397 (1968). doi:10.1107/S0567739468000756

28. Ibers, J.A., Hamilton, W.C.: International tables for X-ray crystallography. vol IV, pp. 71–98. Kynoch Press, Birmingham, England (1974)

29. Cromer, D.T.: Anomalous dispersion corrections computed from self-consistent field relativistic Dirac-Slater wave functions. Acta Crystallogr. **18**, 17–23 (1965). doi:10.1107/S0365110X6500004X

30. Ibers, J.A., Hamilton, W.C.: International tables for X-ray crystallography. vol IV, pp. 148–150. Kynoch Press, Birmingham, England (1974)

31. Baerlocher, Ch., Meier, W.M., Olson, D.H. Atlas of zeolite framework types, Elsevier, Amsterdam (2001)

32. Loewenstein, W.: The distribution of aluminum in the tetra-hedra of silicate and aluminates. Am. Mineral. **39**, 92–96 (1954)

33. Handbook of Chemistry and Physics. 70th ed., pp. F-187. The Chemical Rubber Co., Cleveland, OH, (1989/1990)

34. Bae, M.N., Kim, Y.: Crystal structure of an acetylene sorption Complex of dehydrated Mn(II)-exchanged zeolite Y. Bull. Korean Chem. Soc. **19**, 1095–1098 (1998)

35. Choi, E.Y., Kim, Y., Han, Y.W., Seff, K.: Structure of a cyclopropane sorption complex of dehydrated fully Mn^{2+}-exchanged zeolite X. Microporous Mesoporous Mater. **40**, 247–255 (2000). doi:10.1016/S1387-1811(00)00253-5

36. Jeong, G.H., Kim, Y., Seff, K.: Crystal structures of the NO and NO_2 sorption complexes of fully dehydrated fully Mn^{2+}-exchanged zeolite X (FAU). Microporous Mesoporous Mater. **93**, 12–22 (2006). doi:10.1016/j.micromeso.2006.01.020

37. Bae, M.N., Song, M.K., Kim, Y., Seff, K.: Crystal structure of $Mn_{46}Si_{100}Al_{92}O_{384}\cdot89H_2S$, a hydrogen sulfide sorption complex of fully dehydrated Mn^{2+}-exchanged zeolite X. Microporous Mesoporous Mater. **63**, 21–31 (2003). doi:10.1016/S1387-1811(03)00428-1

38. Stoicheff, B.P.: High resolution Raman spectroscopy of gates: II. Rotational spectra of C_6H_6 and C_6D_6, and internuclear distances in the benzene molecule. Can. J. Phys. **32**, 339–346 (1954)